Soft Matter

PAPER

View Article Online
View Journal | View Issue

Cite this: *Soft Matter*, 2023, **19**, 2902

Effect of temperature on the structure and drug-release behaviour of inclusion complex of β-cyclodextrin with cyclophosphamide: a molecular dynamics study†

Seiga Sakai, Yoshinori Hirano, Yusei Kobayashi and Noriyoshi Arai *

Cyclodextrins (CDs) are suitable drug carriers because of their doughnut-shaped cavities with hydrophilic outer and hydrophobic inner surfaces. Temperature-responsive CD-based drug carriers are expected to be one of the most promising candidates for drug delivery systems. In this study, we performed molecular dynamics simulations of the inclusion complex of β-CD with cyclophosphamide (CP) at temperatures from 300 K to 400 K to investigate the temperature dependency of the release behaviour of CP and structural changes of β-CD in an aqueous solution. We analysed the distance between the centres of mass of β-CD and CP and the radius of gyration of β-CD. The CP molecule was released from the β-CD cavity at 400 K, whereas two different inclusion complexes, partially and completely, were observed at $T < 400$ K. β-CD encapsulating a CP molecule had a more spherical shape and rigidity than β-CD without a CP, and the rigidity of their inclusion complex decreased with increasing temperature. Our findings provide fundamental insights into the behaviours of the β-CD/CP complex and drug release at the molecular level and can facilitate the development of new temperature-responsive drug delivery systems with CD nanocarriers triggered by localised temperature increases using focused ultrasound.

Received 25th November 2022,
Accepted 22nd March 2023

DOI: 10.1039/d2sm01542k

rsc.li/soft-matter-journal

1 Introduction

Cyclophosphamide (CP) is a leading anticancer drug[1,2] that is used to treat most types of cancers, such as multiple myeloma,[3] leukaemia,[4] and breast cancer.[5] CP is a type of active alkylating agent that can form cross-links with and within DNA, resulting in the inhibition of cancer cell growth (*i.e.*, inducing apoptosis/programmed cell death).[6] However, there are risks of serious side effects, such as bone marrow suppression, heart failure, and haemorrhagic cystitis, because alkylating drugs can damage normal cells as well as cancer cells. To overcome this problem, the development of innovative targeted anticancer drugs is essential.

A drug delivery system (DDS) is any technology that adequately delivers drugs to the target disease site and is characterised by time, location, and dosage. Cyclodextrins (CDs) that have doughnut-shaped cavities with hydrophilic outer and hydrophobic inner surfaces have attracted considerable attention as potential drug carriers.[7–10] A significant feature of such cage-type molecules is the formation of an inclusion complex with a drug molecule. Notably, the β-CD molecule containing seven glucopyranose units has desirable features, such as cavity diameter and volume that allow for inclusion of many types of drugs (~6.0–6.5 Å; and ~262 Å^3, respectively) and relatively low cost of production owing to advances in synthetic technology.[11] In the past decade, extensive research on β-CDs and β-CD-drug complexes has been conducted *via* computer simulations[12–18] and experiments[14,18–25] with the goal of developing new DDSs. For instance, a recent experimental study on the inclusion complex of Sulfobutyl-β-CD and Celastrol demonstrated that the formation of the inclusion complex enhances Celastrols intestinal permeability and stability under physiological and biological conditions.[25]

To develop high-performance DDSs, controlled drug release must be achieved, in addition to effective drug loading into β-CD. Accordingly, stimuli-responsive drug carriers based on CD have attracted much attention and have already been extensively studied as "smart" DDSs.[26–28] Various stimuli-responsive systems, including endogenous stimuli (*e.g.* pH,[29,30] enzyme,[31,32] and redox[33,34]) and exogenous stimuli (*e.g.* temperature,[35,36] ultrasound,[37,38] and light[39,40]), have been proposed to achieve foreseeable and controllable drug release. Among these, temperature-responsive systems stand out in manageability, non-invasiveness, and activation of anti-tumour immune

Department of Mechanical Engineering, Keio University, Yokohama, Kanagawa 223-8522, Japan. E-mail: arai@mech.keio.ac.jp

† Electronic supplementary information (ESI) available. See DOI: https://doi.org/10.1039/d2sm01542k

response relative to other methods. As a heating strategy, a localised temperature increase *in situ* by ultrasonic irradiation utilising the amplitude of the wave has been presented.[41–43] In particular, focused ultrasound (FUS) waves can be precisely focused on a target area to produce high local temperatures.[44,45] In the first *in vitro* validation of a temperature-responsive CD-based drug carrier with local heating by FUS, Gourevich *et al.*[37] investigated the effect of FUS-induced local heating on the drug-release behaviour of doxorubicin (Dox) from the CD cavity and showed that Dox can be released by the localised temperature increase using FUS under magnetic resonance imaging guidance.

Molecular dynamics (MD) simulation is a powerful tool for gathering microscopic insights into the behaviours of inclusion complexes and drug release, shedding light on experimental observations, and guiding future DDS applications. To date, many MD simulation studies[16,46–52] on the inclusion complex of β-CD with various drug molecules have been reported. Recently, the structural stability, inclusion process, and thermodynamic properties of CD-drug complexes at a limited range of temperatures have been investigated.[51,52] However, the effect of temperature on the inclusion state of the β-CD/CP complex and the CP release behaviour at the molecular level have not yet been systematically elucidated. This study aimed to gain fundamental insights into the behaviour of the β-CD/CP complex and drug release in the development of ultrasound-mediated targeted drug delivery with CD nanocarriers. To this end, we performed MD simulations of the β-CD/CP inclusion complex in an aqueous solution within a wide temperature range to investigate the effect of temperature on CP release conditions and β-CD structural changes.

2 Model and methods

All MD simulations were performed using the GROMACS 2020.5.[53,54] Fig. 1(a) and (b) show the molecular structures of β-CD and CP, respectively. We used the GLYCAM06 force field[55] for β-CD, general amber force field (GAFF)[56] for CP, and TIP3P force field[57] for water. The partial charges for the CP were calculated at an RHF/6-31G(d) level using Gaussian 16 software (Gaussian Inc.)[58] and the restrained electrostatic potential method. To investigate the effect of CP inclusion on the structural changes of β-CD, we prepared two systems: (i) a single β-CD molecule in water and (ii) β-CD and CP molecules in water. In the β-CD/CP system, the CP molecule was initially positioned close to the centre of the large rim of β-CD, as shown in Fig. 1(c). The distance between the centres of mass of β-CD and CP was set to $d_{cm} \approx 0.90$ nm. All systems were fully solvated with 9,258 water molecules. The edge length of the cubic simulation box was set to $L = 7$ nm, and periodic boundary conditions were applied for all three spatial conditions.

In this study, we simulated the inclusion process at normal temperature ($T = 300$ K) and atmospheric pressure ($P = 0.1$ MPa), and the heating process from 300 to 400 K. For the inclusion process, energy minimisation was initially carried out until the maximum force was reduced to less than 1000 kJ mol^{-1} nm^{-1},

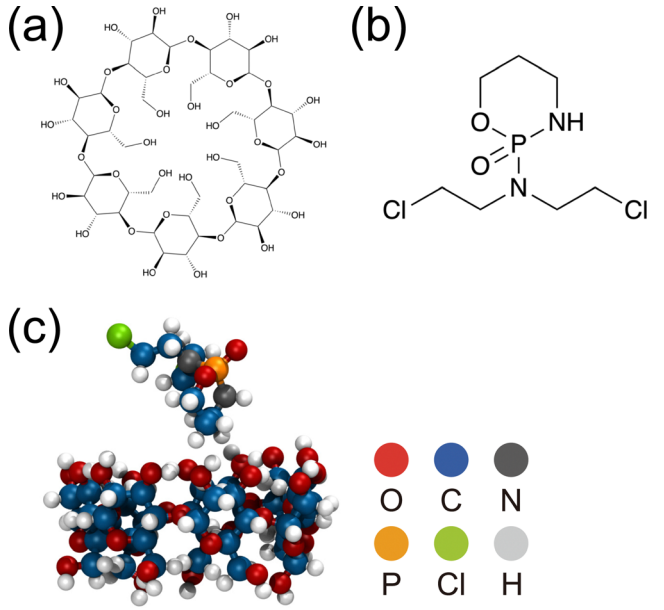

Fig. 1 Molecular structures of (a) β-cyclodextrin (β-CD) and (b) cyclophosphamide (CP). (c) Snapshot of the initial configuration of the β-CD and CP (before inclusion into the β-CD cavity). Snapshot rendered using Visual Molecular Dynamics (version 1.9.4).[59]

using the steepest descent method. Next, *NVT* simulations were performed to relax the system for 0.1 ns, followed by *NPT* simulations for 10 ns. The temperature was fixed using the *V*-rescale temperature coupling method[60] with a time constant of 0.1 ps, and the pressure was controlled using a Parrinello–Rahman barostat[61] with a coupling time constant of 2.0 ps. The equations of motion were integrated using the leapfrog algorithm[62], with a time step of 2.0 fs. The cut-off radii for both the Lennard-Jones and long-range electrostatic interactions were taken as 1.0 nm. The particle mesh Ewald method[63] was used to calculate the long-range electrostatic force. The LINCS algorithm[64] was used to constrain the lengths of all bonds. After the equilibrium simulations at $T = 300$ K and $P = 0.1$ MPa were completed, we started the heating process with a heating rate of 10 K/10 ns using an inclusion state of β-CD/CP as the initial configuration.[65,66] For each temperature, 10 ns equilibrium MD simulations were performed with a time step of 2.0 fs.

3 Results and discussion

First, we performed equilibrium MD simulations at $T = 300$ K and $P = 0.1$ MPa to observe the formation of the inclusion complex of β-CD with CP. For quantitative analysis, we evaluated the inclusion state based on the distance, d_{cm}, between the centres of mass of β-CD and CP. Fig. 2 shows the time evolution of distance between the centres of mass, d_{cm}, of β-CD and CP, and the radius of gyration, R_g, of β-CD. We can see a clear decrease in d_{cm} at $t \approx 4.5$ ns, and the distance remains approximately constant close to the $d_{cm} \lessapprox 0.1$ nm for $t \lessapprox 5.2$ ns. These results indicate that β-CD can completely encapsulate CP at normal temperature and pressure, as reported in a previous

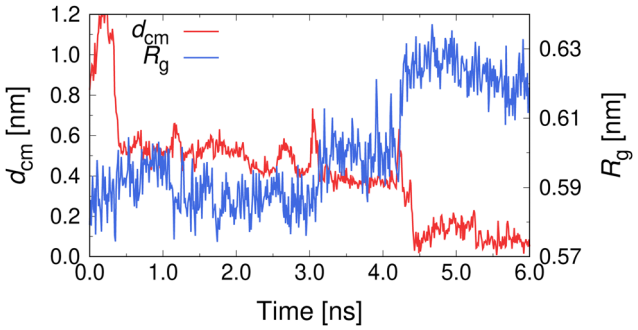

Fig. 2 Time evolution of distance between the centres of mass, d_{cm}, of β-CD and CP and radius of gyration, R_g, of β-CD at T = 300 K and P = 0.1 MPa.

experiment.[67] We also found that R_g of β-CD increased from $R_g \approx 0.59$ nm at $t \lessapprox 3.0$ ns to $R_g \approx 0.62$ nm at $t \lessapprox 4.5$ ns by inclusion of CP into the β-CD cavity.

Next, we performed heating simulations with a heating rate of 10 K/10 ns to investigate the drug-release condition by temperature rise and the effect of temperature on the inclusion state of the β-CD/CP complex. Fig. 3 shows the representative results for d_{cm} as a function of time at T = 310, 330, 350, 380, and 400 K. The representative simulation snapshots for the behaviours of the β-CD/CP complex and drug release during the equilibrium simulation of 10 ns are presented in Fig. S1 of the ESI.† As shown in Fig. 3, we observed the release of CP molecules from the β-CD cavity at T = 400 K. Most β-CD/drug complexes release a drug molecule from the β-CD cavity at T = 50–60 °C[11] however, our results indicate that the β-CD/CP complex is stable at higher temperatures. A recent experimental study of the inclusion complex of podophyllotoxin with β-CD[23] showed that the thermal stability of the encapsulated podophyllotoxin is significantly improved by the cavity of the β-CD. Our results also suggest that inclusion complexation improves the thermal stability of CP. The analysis of the thermal properties of the β-CD/CP complex remains an interesting topic for future work. For $T \geq 380$ K, although d_{cm} slightly increased to $\approx$0.40 nm, the inclusion state was maintained for at least 10 ns. As the temperature increases, the thermal motions of the molecules become larger and more frequent, making the β-CD/CP complex unstable at higher temperatures. We also checked whether any water molecules remained in the cavity of the β-CD/CP complex. The average number of water molecules, N_w, in the β-CD cavity, as shown in Fig. S2 of the ESI.† The cut-off distance from the centres of mass of β-CD to water oxygens was set to 5 Å; based on a previous study.[52] This analysis shows that 1–2 water molecules exist inside the cavity of the β-CD/CP complex in the inclusion state at $T \leq 390$ K. In the single-dispersion state at T = 400 K, the β-CD cavity was occupied by 7 water molecules. To obtain a detailed understanding of the inclusion state of the β-CD/CP complex, we conducted additional simulations for 100 ns at selected temperatures. For each temperature, we performed ten independent simulations to improve the statistics of the MD data. Fig. 4(a) shows the distribution of the distance between the centres of mass of β-CD and CP, $P(d_{cm})$. A distinct peak was observed at $d_{cm} \approx 0.04$ nm for all investigated T. As T increased, the peak at $d_{cm} \approx 0.04$ nm gradually weakened while, a weak peak at $d_{cm} \approx 0.33$ nm appeared. To better demonstrate the difference in the inclusion state of the β-CD/CP complex, we have included representative snapshots of complete inclusion state with d_{cm} = 0.044 nm and partial inclusion state with d_{cm} = 0.326 nm in Fig. 4(b) and (c), respectively. These results indicate that the probability of a partial inclusion state which could cause the release of CP from β-CD under thermal fluctuation increases with increasing T.

In addition to the analysis of the distance between CP and β-CD, a structural analysis of the inclusion states was carried out. Fig. 5(a) shows the probability distribution of the radius of gyration of β-CD, $P(R_g)$, in the inclusion state of the β-CD/CP complex. A distinct peak was observed at $R_g \approx 0.625$ nm for all T values. When increasing the temperature to T = 380 K, the

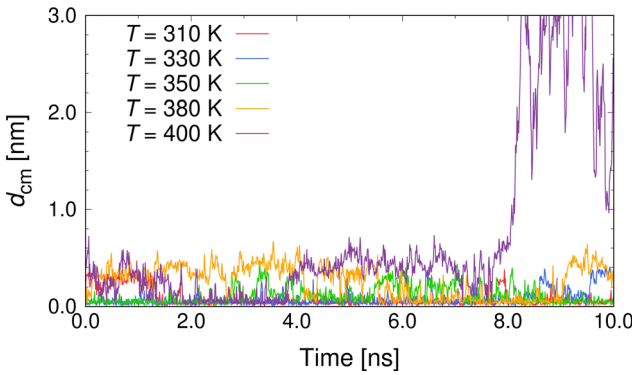

Fig. 3 Distance between the centres of mass, d_{cm}, of β-CD and CP as a function of time for various T, as indicated.

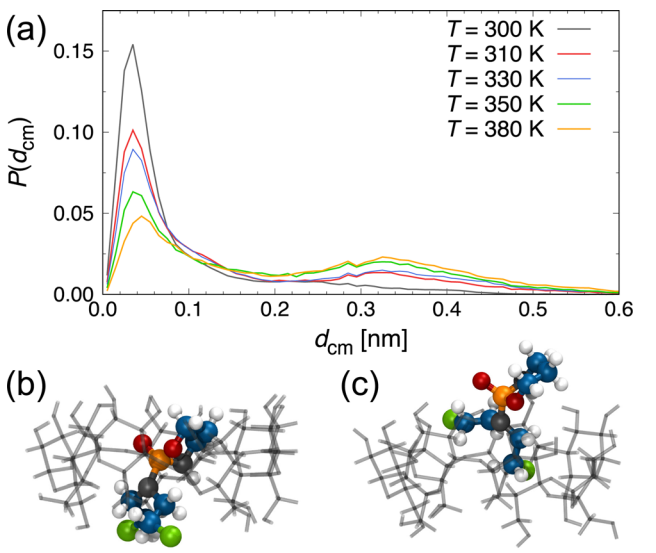

Fig. 4 Distribution, $P(d_{cm})$, of distance between the centres of mass of β-CD and CP in the inclusion state. Representative simulation snapshots of (b) complete inclusion state with d_{cm} = 0.044 nm for T = 300 K and (c) partial inclusion state with d_{cm} = 0.326 nm for T = 380 K.

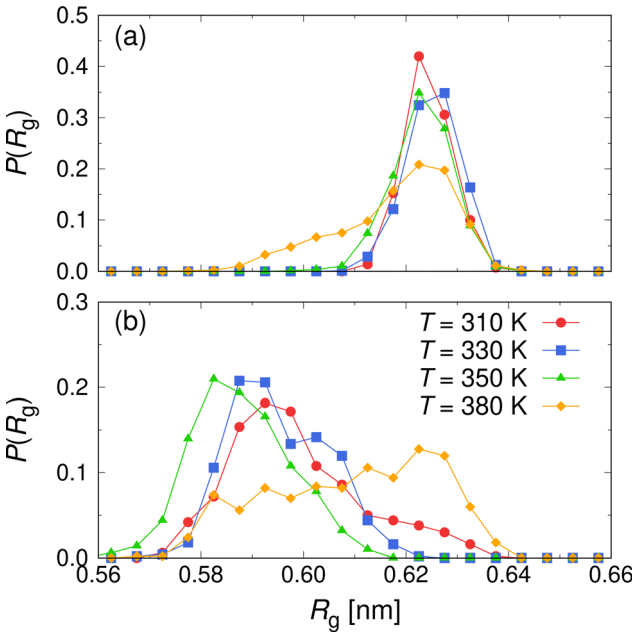

Fig. 5 Probability distribution of the radius of gyration, R_g, of β-CD, $P(R_g)$ in the (a) inclusion state and (b) single-dispersion state.

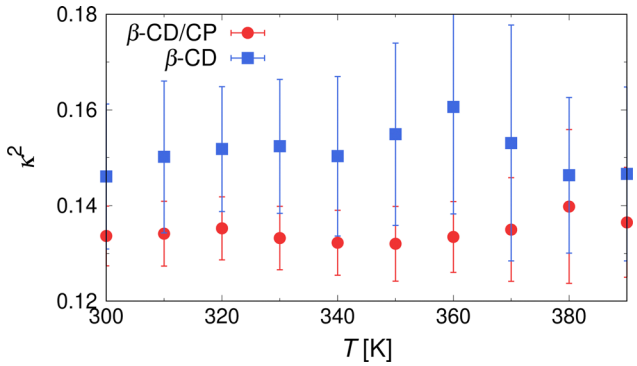

Fig. 6 Relative shape anisotropy, κ^2, as a function of temperature, T, for inclusion (red circles) and single-dispersion state (blue squares).

intensity of this peak obviously decreases, and the distribution of R_g develops a shoulder toward lower values, indicating a decrease in the R_g of β-CD by a transition to a partially occluded state of the β-CD/CP. To confirm that β-CD retained its rigidity upon inclusion of CP into the β-CD cavity, we also performed a heating simulation for a single β-CD solution and computed the distribution of R_g, as shown in Fig. 5(b). Compared with the case of the inclusion state (Fig. 5(a)), broader distributions were observed at each temperature, and the peak of $P(R_g)$ shifted to higher R_g values at T = 380 K. The temperature dependence of $P(R_g)$ of β-CD in the single-dispersion state for all investigated T is shown in Fig. S3 of the ESI.† As an overall trend, we can see the temperature dependence of $P(R_g)$ of β-CD in the single-dispersion state. This behaviour was observed also in previous simulation study.[68] We also conclude that the R_g of β-CD slightly increases, particularly at $T < 360$ K, and β-CD can maintain rigidity by the inclusion of CP into the β-CD cavity. To obtain more details on the structural changes of β-CD, we introduced the relative shape asymmetry parameter, κ^2, defined as

$$\kappa^2 = 1 - 3\frac{G_1G_2 + G_1G_3 + G_2G_3}{(G_1 + G_2 + G_3)^2} \quad (1)$$

where G_1, G_2, and G_3 are the three eigenvalues of gyration tensor G of β-CD. Parameter κ^2 is bounded between values of 0 and 1, which correspond to perfectly spherical and linear shapes, respectively. Fig. 6 shows κ^2 as a function of T, where κ^2 is averaged over all inclusion states (defined as $d_{cm} < 0.40$ nm here, since this value is slightly larger than the peak of $P(d_{cm})$, indicating the partial inclusion state.) found in an MD simulation of 10 ns at each temperature. For comparison, κ^2 for the single-dispersion state was also added to Fig. 6. The error bars in Fig. 6 reflect the standard deviation of κ^2, indicating the shape variability of the β-CD. We found that β-CD that encapsulates a CP molecule shows lower κ^2 values, indicating a more spherical shape than that of the single-dispersion state for all investigated T. In addition, this spherically shaped β-CD was more sterically stabilised, which is also reflected by the small error bars, as confirmed by the results of $P(R_g)$ (Fig. 5).

4 Conclusions

We studied the effect of temperature rise on the release behaviour of cyclophosphamide (CP) and structural changes of β-cyclodextrins (CD) in an aqueous solution *via* molecular dynamics simulations. Under normal temperature and pressure, the formation of the inclusion complex of β-CD with CP was observed, and CP was completely encapsulated by the cavity of β-CD. We also found that the radius of gyration of β-CD was increased by the inclusion of CP into the β-CD cavity. When the inclusion complex of β-CD with CP was gradually heated, the CP molecule was released from the β-CD cavity within 10 ns at T = 400 K. For $T < 400$ K, we observed the existence of two different inclusion complexes: partial and complete inclusion states, based on the distance between the centres of mass of β-CD and CP. As T was increased, the probability of a partially unstable state, which is more vulnerable to temperature increase, could cause the CP to be released from β-CD under thermal fluctuation. Further, we found that β-CD encapsulating a CP molecule has a more spherical shape and rigidity than β-CD without a CP molecule, and the rigidity of their inclusion complex decreases with the increase in T. Our findings provide fundamental insights at the molecular level into the behaviours of the β-CD/CP complex and drug release, and can facilitate the development of ultrasound-mediated targeted drug delivery with CD nanocarriers.

Conflicts of interest

There are no conflicts to declare.

Acknowledgements

The authors are grateful to Dr. Kurokawa (The University of Tokyo) for useful comments on anticancer drugs. Y.K. was

supported by JSPS KAKENHI Grant JP21K20411. This research was partially supported by the Research Grant of Keio Leading-Edge Laboratory of Science & Technology through project number YAL107588.

References

1 O. Colvin, *Curr. Pharm. Des.*, 1999, **5**, 555–560.
2 A. Emadi, R. Jones and R. Brodsky, *Nat. Rev. Clin. Oncol.*, 2009, **6**, 638–647.
3 C. Reeder, D. Reece, V. Kukreti, C. Chen, S. Trudel, J. Hentz, B. Noble, N. Pirooz, J. Spong, J. Piza, V. Zepeda, J. Mikhael, J. Leis, P. Bergsagel, R. Fonseca and A. Stewart, *Leukemia*, 2009, **23**, 1337–1341.
4 C. Tam, S. O'Brien, W. Wierda, H. Kantarjian, S. Wen, K. Do, D. Thomas, J. Cortes, S. Lerner and M. Keating, *Blood*, 2008, **112**, 975–980.
5 M. Levine, V. Bramwell, K. Pritchard, B. Norris, L. Shepherd, H. Abu-Zahra, B. Findlay, D. Warr, D. Bowman, J. Myles, A. Arnold, T. Vandenberg, R. MacKenzie, J. Robert, J. Ottaway, M. Burnell, C. Williams and D. Tu, *J. Clin. Oncol.*, 1998, **16**, 2651–2658.
6 H. Rycenga and D. Long, *Curr. Opin. Pharmacol.*, 2018, **41**, 20–26.
7 F. Hirayama and K. Uekama, *Adv. Drug Delivery Rev.*, 1999, **36**, 125–141.
8 R. Biswas, S. Yang, R. Crichton, P. Adly-Gendi, T. Chen, W. Kopcha, Z. Shi and J. Zhang, *Nanoscale*, 2022, **14**, 4456–4462.
9 V. Doan, J. Lee, R. Takahashi, P. Nguyen, H. Nguyen, V. A. T. Pham, S. Fujii and K. Sakurai, *Polym. J.*, 2020, **52**, 457–466.
10 G. Narayanan, J. Shen, I. Matai, A. Sachdev, R. Boy and A. Tonelli, *Prog. Mater. Sci.*, 2022, **124**, 100869.
11 E. Del Valle, *Process Biochem.*, 2004, **39**, 1033–1046.
12 C. Hanpaibool, T. Chakcharoensap, Arifin, Y. Hijikata, S. Irle, P. Wolschann, N. Kungwan, P. Pongsawasdi, P. Ounjai and T. Rungrotmongkol, *J. Mol. Liq.*, 2018, **265**, 16–23.
13 B. Bezzina, R. Djémil, D. Khatmi, S. Humbel and Y. Carissan, *J. Inclusion Phenom. Macrocyclic Chem.*, 2018, **92**, 115–127.
14 I. González-Méndez, R. Aguayo-Ortiz, K. Sorroza-Martínez, J. Solano, P. Porcu, E. Rivera and L. Dominguez, *Bioorg. Med. Chem.*, 2020, **28**, 115510.
15 F. Mahmoudi and M. Shahraki, *Mol. Syst. Des. Eng.*, 2021, **6**, 643–653.
16 M. Erdös, M. Frangou, T. Vlugt and O. Moultos, *Fluid Phase Equilib.*, 2021, **528**, 112842.
17 A. Oo, K. Kerdpol, P. Mahalapbutr and T. Rungrotmongkol, *J. Mol. Liq.*, 2022, **347**, 118002.
18 A. Cesari, G. Uccello-Barretta, K. Kirschner, M. Pappalardo, L. Basile, S. Guccione, C. Russotto, M. Lauro, F. Cavaliere and F. Balzano, *New J. Chem.*, 2020, **44**, 16431–16441.
19 J. Bezamat, F. Yokaichiya, M. Dias Franco, S. Castro, E. de Paula and L. Cabeça, *J. Drug Delivery Sci. Technol.*, 2020, **55**, 101475.
20 K. Sorroza-Martínez, I. González-Méndez, R. Martínez-Serrano, J. Solano, A. Ruiu, J. Illescas, X. Zhu and E. Rivera, *RSC Adv.*, 2020, **10**, 25557–25566.
21 A. Doan, V. Doan, J. Katsuki, S. Fujii, H. Kono and K. Sakurai, *ACS Omega*, 2022, **7**, 10890–10900.
22 Z. Li, X. Jiang, L. Zhu, F. Chen, H. Liu and L. Ming, *J. Therm. Anal. Calorim.*, 2022, **147**, 11301–11312.
23 W. Yang, L. Yang, F. Li, Y. Zhao, X. Liao, C. Gao, J. Yang and B. Yang, *J. Mol. Struct.*, 2021, **1228**, 129744.
24 B. Várnai, M. Grabarics, Z. Szakács, K. Pagel, M. Malanga, T. Sohajda and S. Béni, *J. Pharm. Biomed.*, 2021, **197**, 113947.
25 S. Shukla, A. Chan, V. Parvathaneni, D. Kanabar, K. Patel, S. Ayehunie, A. Muth and V. Gupta, *J. Mol. Liq.*, 2020, **318**, 113936.
26 B. Tian, Y. Liu and J. Liu, *Carbohydr. Polym.*, 2021, **251**, 116871.
27 X. Yao, J. Mu, L. Zeng, J. Lin, Z. Nie, X. Jiang and P. Huang, *Mater. Horiz.*, 2019, **6**, 846–870.
28 Y. Yuan, T. Nie, Y. Fang, X. You, H. Huang and J. Wu, *J. Mater. Chem. B*, 2022, **10**, 2077–2096.
29 F. Adeli, F. Abbasi, M. Babazadeh and S. Davaran, *J. Nanobiotechnol.*, 2022, **20**, 91.
30 P. Liu and R. Zhang, *Colloids Surf., A*, 2022, **577**, 291–295.
31 Y. Yang, Y.-M. Zhang, Y. Chen, J.-T. Chen and Y. Liu, *Sci. Rep.*, 2016, **6**, 19212.
32 R. Namgung, Y. Mi Lee, J. Kim, Y. Jang, B.-H. Lee, I.-S. Kim, P. Sokkar, Y. Rhee, A. Hoffman and W. Kim, *Nat. Commun.*, 2014, **5**, 3702.
33 X. Chen, Y.-K. Qiu, C. Owh, X. Loh and Y.-L. Wu, *Nanoscale*, 2016, **8**, 18876–18881.
34 Y. Hu, N. Zhao, B. Yu, F. Liu and F.-J. Xu, *Nanoscale*, 2014, **6**, 7560–7569.
35 D. Zhang, C. Yang, Z. Niu, C. Wang, S. Mukherjee, D. Wang, X. Li, R. Liu, J. Gao and Y. Chen, *Langmuir*, 2018, **34**, 11567–11574.
36 Y. Toyoshima, A. Kawamura, Y. Takashima and T. Miyata, *J. Mater. Chem. B*, 2022, **10**, 6644–6654.
37 D. Gourevich, O. Dogadkin, A. Volovick, L. Wang, J. Gnaim, S. Cochran and A. Melzer, *J. Controlled Release*, 2013, **170**, 316–324.
38 C. Wang and F. Du, *Drug Dev. Res.*, 2020, **81**, 585–592.
39 J. Zhang, Z.-H. Zhou, L. Li, Y.-L. Luo, F. Xu and Y. Chen, *Mol. Pharmaceutics*, 2020, **17**, 1100–1113.
40 D. Pacardo, B. Neupane, S. Rikard, Y. Lu, R. Mo, S. Mishra, J. Tracy, G. Wang, F. Ligler and Z. Gu, *Nanoscale*, 2015, **7**, 12096–12103.
41 G. Ter Haar, *Ultrasound Med. Biol.*, 1995, **21**, 1089–1100.
42 K. Suslick, *Ultrasound: its chemical, physical, and biological effects*, Vch Publishers, 1988.
43 C.-H. Fan, Y.-J. Ho, C.-W. Lin, N. Wu, P.-H. Chiang and C.-K. Yeh, *Expert Opin. Drug Delivery*, 2022, **19**, 997–1009.
44 B. Joshi and A. Joshi, *Bioelectronics and Medical Devices*, Woodhead Publishing, 2019, pp. 241–260.
45 D. Xu, L. Wang, S. Cochran and A. Melzer, *J. Ther. Ultrasound*, 2015, **3**, 1–3.
46 F. Garrido, M. Calvelo, R. Garcia-Fandiño and Á. Piñeiro, *Biomolecules*, 2020, **10**, 3.
47 C. Schönbeck, *J. Phys. Chem. B*, 2018, **122**, 4821–4827.
48 K. Jitapunkul, P. Toochinda and L. Lawtrakul, *Molecules*, 2021, **26**, 6784.

49 D. Makieła, I. Janus-Zygmunt, K. Górny and Z. Gburski, *J. Mol. Liq.*, 2018, **262**, 451–459.
50 W. Khuntawee, M. Karttunen and J. Wong-ekkabut, *Phys. Chem. Chem. Phys.*, 2017, **19**, 24219–24229.
51 M. Mojdehi, G. Koli, D. Bolagh, G. Gardeh and S. Hashemianzadeh, *Mol. Syst. Des. Eng.*, 2021, **6**, 80–92.
52 K. Leko, M. Hanževački, Z. Brkljača, K. Pičuljan, R. Ribić and J. Požar, *Chem. Eur.*, 2020, **26**, 5208.
53 H. Berendsen, D. van der Spoel and R. van Drunen, *Comput. Phys. Commun.*, 1995, **91**, 43–56.
54 E. Lindahl, M. Abraham, B. Hess and D. van der Spoel, *GROMACS 2020.5 Source code*, 2021, DOI: **10.5281/zenodo.4420785**.
55 K. Kirschner, A. Yongye, S. Tschampel, J. González-Outeiriño, C. Daniels, B. Foley and R. Woods, *J. Comput. Chem.*, 2008, **29**, 622–655.
56 J. Wang, R. Wolf, J. Caldwell, P. Kollman and D. Case, *J. Comput. Chem.*, 2004, **25**, 1157–1174.
57 W. Jorgensen, J. Chandrasekhar, J. Madura, R. Impey and M. Klein, *J. Chem. Phys.*, 1983, **79**, 926–935.
58 M. J. Frisch, G. W. Trucks, H. B. Schlegel, G. E. Scuseria, M. A. Robb, J. R. Cheeseman, G. Scalmani, V. Barone, G. A. Petersson, H. Nakatsuji, X. Li, M. Caricato, A. V. Marenich, J. Bloino, B. G. Janesko, R. Gomperts, B. Mennucci, H. P. Hratchian, J. V. Ortiz, A. F. Izmaylov, J. L. Sonnenberg, D. Williams-Young, F. Ding, F. Lipparini, F. Egidi, J. Goings, B. Peng, A. Petrone, T. Henderson, D. Ranasinghe, V. G. Zakrzewski, J. Gao, N. Rega, G. Zheng, W. Liang, M. Hada, M. Ehara, K. Toyota, R. Fukuda, J. Hasegawa, M. Ishida, T. Nakajima, Y. Honda, O. Kitao, H. Nakai, T. Vreven, K. Throssell, J. A. Montgomery, Jr., J. E. Peralta, F. Ogliaro, M. J. Bearpark, J. J. Heyd, E. N. Brothers, K. N. Kudin, V. N. Staroverov, T. A. Keith, R. Kobayashi, J. Normand, K. Raghavachari, A. P. Rendell, J. C. Burant, S. S. Iyengar, J. Tomasi, M. Cossi, J. M. Millam, M. Klene, C. Adamo, R. Cammi, J. W. Ochterski, R. L. Martin, K. Morokuma, O. Farkas, J. B. Foresman and D. J. Fox, *Gaussian 16 Revision C.01*, Gaussian Inc, Wallingford CT, 2016.
59 W. Humphrey, A. Dalke and K. Schulten, *J. Mol. Graphics*, 1996, **14**, 33–38.
60 G. Bussi, D. Donadio and M. Parrinello, *J. Chem. Phys.*, 2007, **126**, 014101.
61 M. Parrinello and A. Rahman, *Phys. Rev. Lett.*, 1980, **45**, 1196–1199.
62 P. Allen and D. Tildesley, *Computer Simulations of Liquids*, Oxford University Press, 1987.
63 T. Darden, D. York and L. Pedersen, *J. Chem. Phys.*, 1993, **98**, 10089–10092.
64 B. Hess, *J. Chem. Theory Comput.*, 2008, **4**, 116–122.
65 G. Zhou, T. Zhao, J. Wan, C. Liu, W. Liu and R. Wang, *Carbohydr. Res.*, 2015, **401**, 89–95.
66 W. Khuntawee, T. Rungrotmongkol, P. Wolschann, P. Pongsawasdi, N. Kungwan, H. Okumura and S. Hannongbua, *Carbohydr. Polym.*, 2016, **141**, 99–105.
67 S. Salazar, N. Yutronic, M. Kogan and P. Jara, *Int. J. Mol. Sci.*, 2021, **22**, 6446.
68 K. Kerdpol, J. Kicuntod, P. Wolschann, S. Mori, C. Rungnim, M. Kunaseth, H. Okumura, N. Kungwan and T. Rungrotmongkol, *Polymers*, 2019, **11**, 145.